PERGAMON

International Journal of Solids and Structures 39 (2002) 2189–2201

INTERNATIONAL JOURNAL OF SOLIDS and STRUCTURES

www.elsevier.com/locate/ijsolstr

Spectral element technique for efficient parameter identification of layered media. Part III: viscoelastic aspects

R. Al-Khoury, A. Scarpas *, C. Kasbergen, J. Blaauwendraad

Section of Structural Mechanics, Faculty of Civil Engineering and Geosciences, Delft University of Technology, Stevinweg 1, 2628 CN, Delft, The Netherlands

Received 7 June 2001; received in revised form 11 January 2002

Abstract

This article addresses the issues of wave propagation in elastic–viscoelastic layered systems and viscous parameter identification from non-destructive dynamic tests. A methodology that combines the spectral element technique, for the simulation of wave propagation, with the differential operator technique, for stress–strain relationship in viscoelastic materials, is adopted. The compatibility between the two techniques stems from the fact that both can be treated in the frequency domain, which enables naturally the adoption of Fourier superposition. The mathematical formulation of spectral elements for Burger's viscoelastic material model is highlighted. Also, an inverse procedure for the identification of the material's Young's moduli and complex moduli for layer systems is described. It is shown that the proposed methodology enables the substitution of an expensive laboratory testing procedure for the determination of material complex moduli with non-destructive dynamic testing.

Keywords: Viscoelastic; Spectral element; Wave propagation; Burger's model; Parameter identification; Falling weight deflectometer

1. Introduction

In Part I and II of this series of articles (Al-Khoury et al., 2001a, 2001b, Part I and II), detailed formulations for wave motions and parameter identifications in linear elastic multi-layer systems were presented. Because many engineering materials exhibit viscoelastic behavior, the method is extended in this article, Part III, to the case of multi-layer systems consisting of both linear elastic and viscoelastic material layers. Emphasis is placed on studying wave motion in a Burger type viscoelastic material, and on identifying the material complex moduli. A typical example of such a material is asphalt concrete.

Viscosity affects the propagation of waves in viscoelastic media in a rather significant manner. The solution of the wave propagation in linear viscoelastic solids can be obtained from that of the corresponding elastic one by replacing Hooke's law with its corresponding viscoelastic stress–strain relationship.

* Corresponding author. Fax: +31-15-278-5767.
E-mail address: a.scarpas@ct.tudelft.nl (A. Scarpas).

0020-7683/02/$ - see front matter
PII: S0020-7683(02)00079-3

In general two different formulations are used to describe the stress–strain relations of viscoelastic materials (Findley et al., 1976):

(a) The differential operator method, in which the stress–strain relationship is expressed as

$$P\sigma_{ij} = Q\varepsilon_{ij} \tag{1}$$

where P and Q are differential operators.

(b) The hereditary integrals method, in which the stress–strain relationship is expressed as

$$\sigma(t) = \int_0^t Y(t-t')\left[\frac{\partial\varepsilon(t')}{\partial t'}\right]\mathrm{d}t' \tag{2}$$

where $Y(t)$ is the relaxation modulus function and t' is the time at which the response strain starts.

Even though both formulations are equivalent to each other, their suitability to solve viscoelastic problems is case dependent. The integral method is able to describe time dependent constitutive models more generally, however, it usually leads to complicated formulations that are less suitable for numerical calculations.

Normally solutions to Eqs. (1) and (2) are done by the application of the Laplace transform. Although the forward Laplace transforms of the viscoelastic solutions can be obtained in a simple manner, it results to rather complicated complex inversion integrals. These integrals are, in many cases, difficult to evaluate analytically as well as numerically. Achenbach (1975) has shown that it is possible to invert the transforms in a relatively simple manner only for the rather special case that the relaxation functions in bulk and in shear show the same time dependence.

In this article, a methodology that combines the spectral element technique (Doyle, 1997), for the simulation of wave propagation in layered systems, with the differential operator technique, Eq. (1), for stress–strain relations in viscoelastic Burger's materials, is adopted. These techniques form a sound combination because the solutions involved, in both methods, can be treated at a particular harmonic (frequency) level. In the spectral element method, the general solution of the wave equations begins with particular solutions of harmonic waves of the form

$$\varphi(\mathbf{x},t) = \widehat{\varphi}(\mathbf{x},\omega)\mathrm{e}^{\mathrm{i}\omega t} \tag{3}$$

In the differential operator technique, the stress–strain relation, Eq. (1), for a viscoelastic material subjected to a harmonic excitation can be expressed as

$$(\mathrm{i}\omega)P\sigma_{ij}\mathrm{e}^{\mathrm{i}\omega t} = (\mathrm{i}\omega)Q\varepsilon_{ij}\mathrm{e}^{\mathrm{i}\omega t} \tag{4}$$

By employing Eq. (4) into (3) the equation of motion in a viscoelastic medium can be solved at each frequency. For a transient case, the general solution to the wave propagation problem can then be obtained by summing over all harmonic waves.

The spectral element technique combines the exact solution of wave motions with the finite element organization of the system matrices. Because waves are described exactly in the spectral element, one element is sufficient to describe a whole layer without the need for subdivisions. Consequently, the size of the mesh of a layered medium is only as large as the number of the layers involved. This reduces the computational requirements dramatically.

Also near-to-intermediate boundary field conditions are considered. Consequently, the solution to the spatial domain can be carried out by means of a series summation. Such a solution avoids the inconvenience of the conventional infinite integration involved in the solution of far field problems. Series summations contribute to the computational efficiency and robustness. It is the computational efficiency of the

spectral element, and the robustness of the series summation, which make the proposed technique attractive for solving inverse problems.

In this article, aspects of the forward calculation of wave propagation in viscoelastic Burger's material layers and inverse calculation of the viscoelastic parameters are presented. As an application, numerical examples are presented for the simulation of wave propagation in a pavement structure as a result of the dynamic action of the non-destructive falling weight deflectometer (FWD) test (van Gurp, 1995). FWD is a commonly used test for pavement quality evaluation studies. Also, the utilization of the above results for the identification of the layer viscoelastic parameters is discussed.

2. Spectral elements for a viscoelastic medium

The formulation of a spectral element begins from the derivation of the equations of motion. The derivation of the equations of motion in a viscoelastic solid follows the same procedure as that of the linear elastic and can be expressed (Kolsky, 1963) as

$$\left\{\tilde{\lambda}(t)+\tilde{\mu}(t)\right\}\nabla\nabla\cdot\mathbf{u}+\tilde{\mu}(t)\nabla^2\mathbf{u}=\rho\ddot{\mathbf{u}} \tag{5}$$

in which $\mathbf{u}$ is the displacement vector, ρ is the mass density, ∇ indicates a vector differential operator; $\nabla\cdot\mathbf{u}$ is the divergence of $\mathbf{u}$ and $\nabla^2\mathbf{u}$ is the vector Laplacian of $\mathbf{u}$, and $\tilde{\lambda}(t)$ and $\tilde{\mu}(t)$ are the viscoelastic material parameters. These parameters can be determined from the viscoelastic stress–strain relationship, which can be expressed in terms of the differential operators P and Q as

$$P\sigma_{ij}=Q\varepsilon_{ij} \tag{6}$$

This relation is also called the *analogy* relation in correspondence with the elastic relations. The operators P and Q of Eq. (6) may be expressed as

$$P\equiv\sum_k p_k\frac{\partial^k}{\partial t^k},\qquad Q\equiv\sum_l q_l\frac{\partial^l}{\partial t^l} \tag{7}$$

where the p's and the q's are material constants and k and l are indices, which depend on the material model. Upon substituting Eq. (7) into Eq. (6) and by use of Fourier transformation, the spectral form of the stress–strain relationship can be expressed as

$$\left\{\sum_k p_k(\mathrm{i}\omega)^k\right\}\widehat{\sigma}_{ij}=\left\{\sum_l q_l(\mathrm{i}\omega)^l\right\}\widehat{\varepsilon}_{ij} \tag{8}$$

where the "hat" indicates that the formulation is in the frequency domain.

Also, by applying Fourier transformation to Eq. (5), the spectral form of the wave motion can be expressed as

$$\{\lambda^*(\omega)+\mu^*(\omega)\}\nabla\nabla\cdot\widehat{\mathbf{u}}+\mu^*(\omega)\nabla^2\widehat{\mathbf{u}}+\omega^2\rho=0 \tag{9}$$

where $\lambda^*(\omega)$ and $\mu^*(\omega)$ are the complex Lame's constants corresponding to the differential operators $\tilde{\lambda}(t)$ and $\tilde{\mu}(t)$ respectively. $\lambda^*(\omega)$ and $\mu^*(\omega)$ can be determined from Eq. (6) for any specific viscoelastic material model. Later in this article $\lambda^*(\omega)$ and $\mu^*(\omega)$ will be derived for Burger's material model.

An elegant way for solving Eq. (9) is by means of Helmholtz decomposition, in which the displacement field can be expressed as the sum of the gradient of a scalar potential φ and the curl of a vector potential $\boldsymbol{\psi}$ as

$$\mathbf{u}=\nabla\varphi+\nabla\times\boldsymbol{\psi} \tag{10}$$

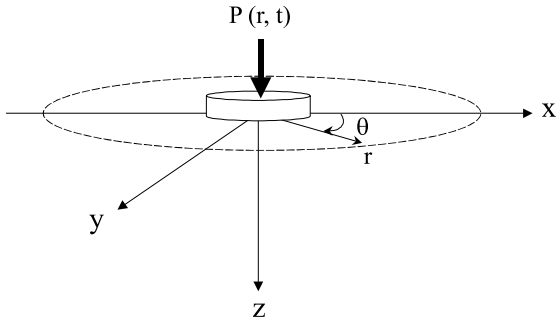

Fig. 1. Axi-symmetric system subjected to a circular load.

For an axially symmetric system, Fig. 1, the vector potential $\boldsymbol{\psi}$ has a component ψ_θ only. This simplifies the solution of the problem to solving only for scalar potentials. For convenience of notation, ψ will be written instead of ψ_θ. Denoting the displacement components in r and z-directions by u_r and u_z respectively, the relations between the displacement components and the potentials are:

$$u_r = \frac{\partial \varphi}{\partial r} - \frac{\partial \psi}{\partial z}, \qquad u_z = \frac{\partial \varphi}{\partial z} + \frac{1}{r}\frac{\partial (r\psi)}{\partial r} \tag{11}$$

and the relevant stresses are

$$\sigma_{zz} = (\lambda + 2\mu)\frac{\partial u_z}{\partial z} + \frac{\lambda}{r}\frac{\partial (ru_r)}{\partial r}, \qquad \tau_{zr} = \mu\left(\frac{\partial u_r}{\partial z} + \frac{\partial u_z}{\partial r}\right) \tag{12}$$

Substituting Eq. (10) into Eq. (9) leads to uncoupled partial differential equations for the longitudinal wave and the transverse wave as

$$-\omega^2 \widehat{\varphi} = [c_p^*(\omega)]^2 \left(\frac{\partial^2 \widehat{\varphi}}{\partial r^2} + \frac{1}{r}\frac{\partial \widehat{\varphi}}{\partial r} + \frac{\partial^2 \widehat{\varphi}}{\partial z^2}\right) \tag{13}$$

$$-\omega^2 \widehat{\psi} = \left[c_s^*(\omega)\right]^2 \left(\frac{\partial^2 \widehat{\psi}}{\partial r^2} + \frac{1}{r}\frac{\partial \widehat{\psi}}{\partial r} + \frac{\partial^2 \widehat{\psi}}{\partial z^2} - \frac{\widehat{\psi}}{r^2}\right) \tag{14}$$

where

$$c_p^*(\omega) = \left(\frac{\lambda^*(\omega) + 2\mu^*(\omega)}{\rho}\right)^{1/2} \quad \text{and} \quad c_s^*(\omega) = \left(\frac{\mu^*(\omega)}{\rho}\right)^{1/2} \tag{15}$$

define the longitudinal and transverse complex wave velocities respectively. The wave number for the longitudinal and the transverse waves are then

$$k_p^* = \omega\left(\frac{\rho}{\lambda^*(\omega) + 2\mu^*(\omega)}\right)^{1/2} \quad \text{and} \quad k_s^* = \omega\left(\frac{\rho}{\mu^*(\omega)}\right)^{1/2} \tag{16}$$

respectively. Apparently the wave numbers are complex which implies that the amplitude decreases with increasing distance and the attenuation rate depends on the frequency.

The solutions of the wave equations (13) and (14) can be expressed (Al-Khoury et al., 2001a, Part I) as

$$\widehat{\varphi}(r, z, \omega) = A e^{i\xi^* z} J_0(\eta r) \tag{17}$$

$$\widehat{\psi}(r,z,\omega) = B\mathrm{e}^{-\mathrm{i}\xi^* z}J_1(\eta r) \tag{18}$$

in which A and B are the wave amplitudes determined from the boundary conditions, J_0 and J_1 are the Bessel functions of the first kind, ω is the angular frequency, η is the wave number in the radial direction and ξ^* and ζ^* are the complex longitudinal and transverse wave numbers in the vertical direction, defined as

$$\xi^* = (k_p^{*2} - \eta^2)^{1/2} \quad \text{and} \quad \zeta^* = (k_s^{*2} - \eta^2)^{1/2} \tag{19}$$

respectively. The spectrum relations, Eq. (16), with their corresponding wave number relations, Eq. (19), constitute the departure from the elastic case.

Then, following the procedures presented in Part I of this series of articles, a layer spectral element and a half-space spectral element can be formulated. The stiffness matrices for a viscoelastic material of both types of elements are listed in the Appendix A.

In the z-direction the layer spectral element is described by two nodes, Fig. 2, and the half-space element is described by one node. In the radial direction, the element is assumed to simulate near-to-intermediate fields. Here, a finite medium with a boundary condition

$$\widehat{u}(r, z = \mathrm{cnt}) = 0; \qquad r = R \tag{20}$$

is considered, in which R is some distance, faraway from the source, at which waves are known a priori to vanish. This condition represents a homogenous boundary condition at $r = R$. The imposition of such a condition will lead inevitably to a series summation of the form

$$u(r,z,\eta_m,\omega_n) = \sum_{m=1}^{\infty} \widehat{G}_{mn}(z)J_v(\eta_m r) \tag{21}$$

where $\widehat{G}_{mn}(z)$ is a function of z, and $J_v(\eta_m r)$ is a function r.

In case of a transient force $P(r,t)$, Fig. 1, with a spatial distribution $S(r)$ and a time variation $F(t)$, the in-time force–displacement relationship can be obtained by

$$u(r,z,t) = \sum_n \sum_m \widehat{G}_{mn}(z)\widehat{F}_m J_v(\eta_m r)\widehat{F}_n \mathrm{e}^{\mathrm{i}\omega_n t} \tag{22}$$

where $\widehat{G}_{mn}(z)J_v(\eta_m r)$ represents the transfer function of the system obtained from the stiffness matrix inversion, $\widehat{F}_m$ is the Fourier–Bessel coefficients of $S(r)$ and $\widehat{F}_n$ denotes the fast Fourier coefficients of $F(t)$. The Fourier coefficient $\widehat{F}_n$ can be obtained numerically by means of the forward fast Fourier transforms (FFT) (Brigham, 1998). The Bessel coefficient $\widehat{F}_m$, on the other hand, can be determined analytically. Quantification of $\widehat{F}_n$ and $\widehat{F}_m$ for a typical FWD load pulse duration and shape are presented in Part I.

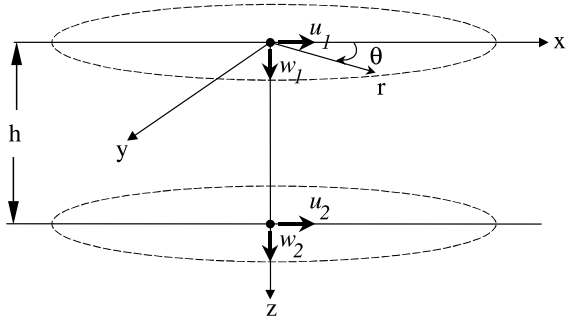

Fig. 2. Axi-symmetric spectral layer element.

3. Spectral simulation of Burger materials

Usually in describing the viscoelastic behavior of a material, combination of springs and dashpots are utilized. Some of the well known models are Maxwell, Voigt (Kelvin), Standard Solid and Burger. Usually the Voigt's model is utilized to simulate viscous damping in materials. In such cases the elastic modulus is replaced by the complex modulus

$$E^* = E(1 + \mathrm{i}\omega\xi_\mathrm{d}) \tag{23}$$

in which the damping ratio $\xi_\mathrm{d} = \eta/E$ with η the dashpot constant and E the spring constant. For many engineering materials such kind of damping is adequate for simulation of the viscous retardation forces. However, for asphaltic materials, Burger's model is commonly utilized (Huang, 1993).

Burger's model (Shames and Cozzarelli, 1992), Fig. 3, simulates the material behavior by a combination of a Maxwell and a Kelvin model in series. The Maxwell model consists of a Hookean element with a linear spring constant E_1 connected in series with a Newtonian element with viscosity coefficient η_1. The Kelvin model consists of a Hookean and a Newtonian element connected in parallel with constants E_2 and η_2 respectively.

The stress–strain relationship for Burger's model under uniaxial compression/tension is expressed as

$$\sigma + \left(\frac{\eta_1}{E_1} + \frac{\eta_1}{E_2} + \frac{\eta_2}{E_2}\right)\dot{\sigma} + \frac{\eta_1\eta_2}{E_1E_2}\ddot{\sigma} = \eta_1\dot{\varepsilon}\frac{\eta_1\eta_2}{E_2}\ddot{\varepsilon} \tag{24}$$

From Eq. (24) it can be shown that the operator pair of Eq. (7) (in tension/compression) for Burger's model is

$$P^E = \left(P_0^E + P_1^E\frac{\partial}{\partial t} + P_2^E\frac{\partial^2}{\partial t^2}\right) \quad \text{and} \quad Q^E = q_1^E\frac{\partial}{\partial t} + q_2^E\frac{\partial^2}{\partial t^2} \tag{25}$$

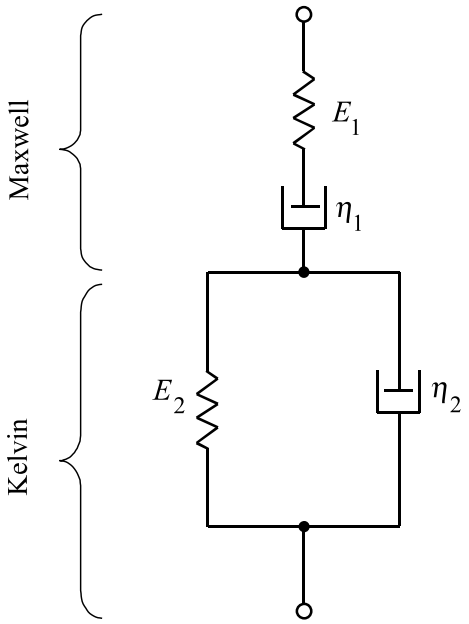

Fig. 3. Burger's model.

in which $P_0^E = 1$, P_1^E and P_2^E are the coefficients of $\dot{\sigma}$ and $\ddot{\sigma}$ in Eq. (24) respectively, and q_1^E and q_2^E are the coefficient of $\dot{\varepsilon}$ and $\ddot{\varepsilon}$ in Eq. (24) respectively.

Applying the Fourier transform to Eq. (24), i.e. substituting $\partial/\partial t$ with $\mathrm{i}\omega$ and $\partial^2/\partial t^2$ with $-\omega^2$, and by using the analogy relation for E, lead to:

$$E^*(\omega) = \frac{\omega^2\left[P_1^E q_1^E - q_2^E\left(1 - P_2^E\omega^2\right)\right] + \mathrm{i}\omega\left[P_1^E q_2^E\omega^2 - q_1^E\left(1 - P_2^E\omega^2\right)\right]}{P_1^E\omega^2 + \left(1 - P_2^E\omega^2\right)^2} \tag{26}$$

which is known as the complex modulus of Burger's model. This modulus can be obtained from uniaxial frequency sweep tests on a cylindrical specimen. As an alternative, as it will be shown later, this modulus can be obtained from dynamic non-destructive testing of structures, which can be of importance in road engineering.

From Eq. (26), the complex shear modulus and the complex Lame's constant can be determined as

$$\mu^*(\omega) = \frac{3K\left(\mathrm{i}\omega q_1^E - \omega^2 q_2^E\right)}{9K(1 + \mathrm{i}\omega P_1^E - \omega^2 P_2^E) - \mathrm{i}\omega q_1^E + \omega^2 q_2^E} \tag{27}$$

and

$$\lambda^*(\omega) = K - \tfrac{2}{3}\mu^*(\omega) \tag{28}$$

respectively, with K being the bulk modulus. Then, by substituting Eq. (27) into the stiffness matrices, Eqs. (A.1) and (A.2), layer and half-space spectral elements for Burger's material can be obtained.

Here the material is assumed to exhibit elastic compressibility for bulk behavior ($\sigma_{ii} = 3K\varepsilon_{ii}$) and a Burger-type behavior under multi-dimensional distortion ($s_{ij} = 2\mu^*(\omega)e_{ij}$). For such a material the variations of the real and imaginary parts of the complex shear modulus with frequency are shown in Fig. 4. It can be seen that this material behaves like a fluid ($|\mu^*| = 0$) at zero frequency, after which the shear modulus starts to increase until it reaches to the elastic shear modulus asymptotically.

The variation of Poisson's ratio with frequency is shown in Fig. 5. It can be seen that at zero frequency Burger's model behaves like a pure incompressible fluid and with increasing frequency the compressibility increases.

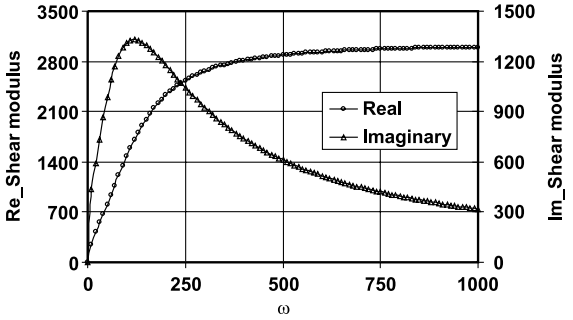

Fig. 4. The real and imaginary parts of the complex shear modulus of a viscoelastic material with $K = 8100$ MPa, $E_1 = 8100$ MPa, $E_2 = 4050$ MPa, $\eta_1 = 200$ MPa s and $\eta_2 = 150$ MPa s.

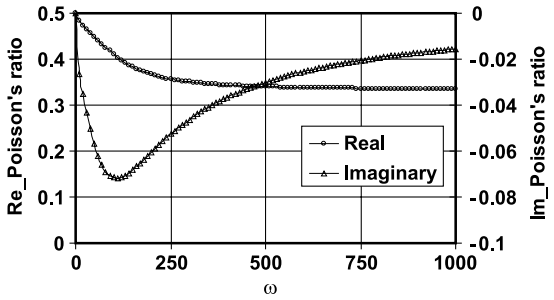

Fig. 5. The real and imaginary parts of the complex Poisson's ratio of a viscoelastic material with $K = 8100$ MPa, $E_1 = 8100$ MPa, $E_2 = 4050$ MPa, $\eta_1 = 200$ MPa s and $\eta_2 = 150$ MPa s.

4. Numerical examples

In this section some numerical analyses are presented to describe the effects of viscosity on wave propagation in layered systems.

As an example, a pavement structure consisting of a top layer of asphalt concrete 100 mm thick, a granular subbase layer 300 mm thick and a subgrade layer of infinite thickness was simulated. The viscoelastic parameters are shown in Table 1 (Hopman, 1996). The pavement was subjected to a bell shape pulse of 50 ms duration (frequency spectrum ranging between 0 and 100 Hz.) and 0.707 MPa stress amplitude over a loaded area of 150 mm radius. The spectral element mesh consisted of three elements only with each element representing a specific material layer; asphalt, subbase and subgrade.

Three different analyses were conducted: in the first it was assumed that all layer materials were elastic, in the second, only the asphalt material was assumed viscoelastic and in the third, all layer materials were assumed viscoelastic. For the elastic layer materials analysis, E_1 of Table 1 was utilized.

The computed vertical displacements at the center of the load application for all three analyses are shown in Fig. 6. The results can easily be interpreted by use of Fig. 4. It can be seen that due to Burger low stiffness at low frequencies, larger displacements are generated with increasing number of the viscoelastic layers. Also, due to viscoelasticity, delayed unloading can clearly be noticed.

To examine the effect of Poisson's ratio, two different analyses were conducted. The first was with constant Poisson's ratio and the second with Poisson's ratio varying with frequency. Fig. 7 shows the vertical displacements directly under the load. The computational results can be interpreted by use of Fig. 5, which shows that at low frequencies, the material behaves more like an incompressible fluid. This results to the increase of its bulk modulus, and hence to a smaller deformation. With increasing frequency the material starts to behave like that of the constant Poisson case.

These examples indicate that at some situations and in particular at higher temperatures, the viscous response of asphalt pavements to dynamic loads should be taken into consideration.

Table 1
Elastic and viscoelastic layer material parameters

Material	E_1 (MPa)	E_2 (MPa)	η_1 (MPa s)	η_2 (MPa s)	K (MPa)	ρ (Kg/m^3)
Asphalt	8100	4050	200	150	8100	2300
Subbase	10 800	13 500	500	1000	10 800	2000
Subgrade	100	50 000	1000	1000	100	1500

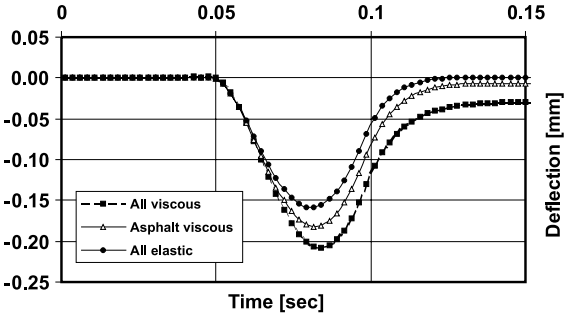

Fig. 6. Wave propagation in a three-layer pavement structure with varying viscosity contribution.

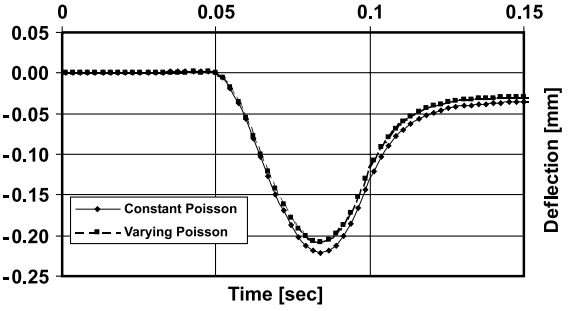

Fig. 7. Effect of layer material Poisson's ratio on pavement response.

5. Elastic–viscoelastic parameter identification

One of the main advantages of the spectral element technique is its suitability for solving inverse problems. In Part II of this series of publications, a procedure for the identification of elastic parameters in layered media has been developed. Here, the procedure is extended to account for the identification of the viscoelastic parameters.

For a linear viscoelastic system, the experimental transfer function $\widehat{G}(\omega_n)$ at a sensor location s, for a given frequency ω_n, can be obtained as

$$\{\widehat{G}_s(\omega_n)\}_{\text{experimental}} = \frac{\widehat{u}_s(\omega_n)}{\widehat{P}(\omega_n)} \tag{29}$$

in which $\widehat{u}_s(\omega_n)$ is the measured displacement at sensor s and $\widehat{P}(\omega_n)$ is the measured force.

Theoretically, on the other hand, $\widehat{G}(\omega_n)$ can be obtained from the spectral element formulation. From Eq. (22) it is obvious that the transfer function at location s can be expressed as

$$\{\widehat{G}_s(\omega_n)\}_{\text{theoretical}} = \sum_m \widehat{G}_{mn}(z) J_0(\eta_m r_s) \tag{30}$$

By relating the theoretical transfer functions with those obtained from the measurements, the system objective function can be constructed as

$$q(\mathbf{x}) = |\widehat{G}_s(\omega_n)|_{\text{experimental}} - \left| \sum_m \widehat{G}_{mn}(z) J_0(\eta_m r_s) \right|_{\text{theoretical}} \approx 0 \tag{31}$$

in which $\mathbf{x}$ represents the vector of the unknown variables such as layer elastic moduli and the viscous parameters, e.g. E_1, E_2, η_1 and η_2 of the Burger's model.

Eq. (31) is a system of multi-dimensional non-linear equations. Solution of such a system can be done by means of minimization techniques. The Modified Powell hybrid algorithm (Press et al., 1986) for solving a non-constrained system of non-linear simultaneous equations with a finite-difference Jacobian has been utilized in this investigation. (In Part II, three different minimization techniques have been utilized for solving the system objective function.)

In road engineering, Burger's model is utilized for the simulation of the viscoelastic behavior of asphalt materials (Hopman, 1996). Such analysis requires data about Burger parameters E_1, E_2, η_1 and η_2, which are necessary for the calculation of the material complex modulus, Eq. (26). These parameters are usually obtained from laboratory frequency sweep tests. Such kind of testing, in addition to being expensive, requires specimens cored out of the road pavement. The specimen coring procedure aggravates traffic congestion conditions and renders viscoelastic analyses less attractive for road authorities.

As an alternative, as it is proposed here, the complex modulus is determined from the measured data of non-destructive tests and in particular from the FWD test. The proposed procedure allows the determination of the complex modulus without a priori knowledge of Burger's parameters. In Eq. (31) the complex modulus is described as

$$E^*(\omega) = E_{\mathrm{Re}} + \mathrm{i}E_{\mathrm{Im}} \tag{32}$$

in which E_{Re} is the real part of the complex modulus, often called the storage modulus and, E_{Im} is the imaginary part of the complex modulus, often called the loss modulus. Solving Eq. (31) will result in the estimation of both E_{Re} and E_{Im}, which can be used in forward viscoelastic analysis.

At this stage of investigation and for the sake of verifying the mathematical derivations and computer implementation of the developed viscous parameter identification procedure, only computed (not contaminated) data was utilized. For this reason, results of FWD forward analyses for the pavement structure with the properties presented in Table 1 were utilized. The vertical displacements at typical sensor locations (radial distances from $r = 0$ to 1800 mm) are shown in Fig. 8.

The displacement data together with the applied load data were used as input for back calculating the material elastic moduli of the subbase and subgrade layers and the complex moduli (at different frequencies) of the asphalt layer.

Table 2 shows the actual parameters as were input in the forward analysis and the back calculated parameters. The actual complex moduli at different frequencies were calculated by means of Eq. (26) and the back calculated are computed by the inverse model without a priori knowledge about the Burger internal parameters. It can be seen that the back calculated moduli are almost identical to the actual ones. The initial guesses (seed values) of the unknown parameters were around 20% of the actual values. The number of iterations needed for the backcalculation of the elastic and complex moduli were ranging between 20 and 40. In an Intel 300 MHz PC, each iteration takes around 1 s.

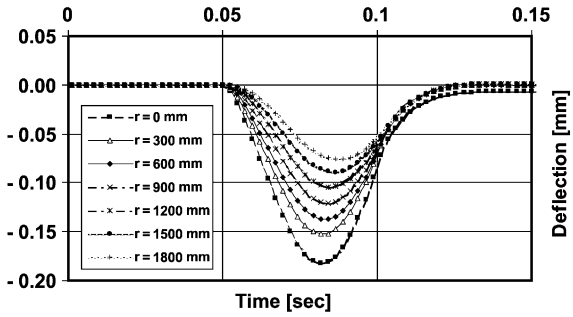

Fig. 8. Vertical displacements at typical sensor locations.

Table 2
Forward and inverse calculation of elastic and viscoelastic material moduli

Frequency (Hz)	Layer	Forward calculation			Inverse calculation		
		E_mod. (MPa)	$E^*(\omega)$ from Eq. (26)		E_mod. (MPa)	$E^*(\omega)$	
			E_{Re}	E_{Im}		E_{Re}	E_{Im}
20	Asphalt		6840.75	2680.60		6840.68	2680.66
	Subbase	10 800			10 799		
	Subgrade	100			99		
25	Asphalt		7251.78	2277.73		7251.79	2277.71
	Subbase	10 800			10 799		
	Subgrade	100			99		
30	Asphalt		7495.12	1961.27		7495.17	1961.34
	Subbase	10 800			10 799		
	Subgrade	100			99		

The significance of this inverse procedure is that the inverse model does not rely on a specific viscoelastic model, such as Burger, Kelvin, Standard Solid, etc. Instead it computes the complex moduli directly. As mentioned earlier, this is important for engineering purposes because it substitutes determination of the viscous parameters via expensive laboratory tests with a relatively inexpensive non-destructive test.

6. Conclusions

The combination between the spectral element technique for wave propagation analysis in layered systems and the differential operator technique for stress–strain relationships in viscoelastic materials has the following advantages:

1. Both techniques can be treated in the frequency domain, and hence their incorporation allows naturally the utilization of the Fourier superposition method for solving transient problems.
2. The double Fourier summation (Fourier–Bessel series for the spatial domain and FFT for the time-frequency domain) over frequency and wave number alleviates the inconvenience of the numerical implementation of the infinite integrals that usually result from adopting other techniques.
3. The spectral element feature of exact solution of wave propagation in a layer element in combination with the finite element organization of multi-layers results to computationally efficient formulations suitable for computer codes. This makes the proposed method appropriate for utilization in iterative schemes for solving inverse problems.
4. The proposed methodology leads to an elegant approach for the determination of material's Young's moduli and viscous complex moduli from the results of non-destructive dynamic tests. In road engineering, this can be of practical importance because it avoids the inconvenience of coring specimens from road pavements and expensive laboratory test procedures.

Acknowledgements

The research project is partially funded by the European Commission under the Standards, Measurements and Testing programme of the 4th Framework under project name "SpecifiQ".

Appendix A

Stiffness matrix for an axi-symmetric viscoelastic layer spectral element is:

$$\widehat{k}_{mn} = \begin{bmatrix} k_{11mn} & k_{12mn} & k_{13mn} & k_{14mn} \\ & k_{22mn} & -k_{14mn} & k_{24mn} \\ & & k_{11mn} & -k_{12mn} \\ \text{sym} & & & k_{22mn} \end{bmatrix} \tag{A.1}$$

where

$$k_{11mn} = \frac{\mu^*(\omega_n)}{\Delta_{mn}} \left\{ \mathrm{i}\xi^*_{mn} \left(\zeta^{*^2}_{mn} + \eta^2_m \right) \left(\eta^2_m Q_{12} Q_{21} + \xi^*_{mn} \zeta^*_{mn} Q_{11} Q_{22} \right) \right\}$$

$$k_{12mn} = \frac{\mu^*(\omega_n)}{\Delta_{mn}} \left\{ \eta_m \xi^*_{mn} \zeta^*_{mn} \left(-\zeta^{*^2}_{mn} + 3\eta^2_m \right) \left(Q_{12} Q_{22} - 4\mathrm{e}^{-\mathrm{i}\xi^*_{mn} h} \mathrm{e}^{-\mathrm{i}\zeta^*_{mn} h} \right) - \eta_m Q_{11} Q_{21} \left(\eta^2_m \zeta^{*^2}_{mn} - \eta^4_m - 2\xi^{*^2}_{mn} \zeta^{*^2}_{mn} \right) \right\}$$

$$k_{13mn} = \frac{\mu^*(\omega_n)}{\Delta_{mn}} \left\{ -2\mathrm{i}\xi^*_{mn} \left(\zeta^{*^2}_{mn} + \eta^2_m \right) \left(\eta^2_m \mathrm{e}^{-\mathrm{i}\xi^*_{mn} h} Q_{21} + \xi^*_{mn} \zeta^*_{mn} \mathrm{e}^{-\mathrm{i}\zeta^*_{mn} h} Q_{11} \right) \right\}$$

$$k_{14mn} = \frac{\mu^*(\omega_n)}{\Delta_{mn}} \left\{ 2\xi^*_{mn} \zeta^*_{mn} \left(\zeta^{*^2}_{mn} + \eta^2_m \right) \left(\mathrm{e}^{-\mathrm{i}\xi^*_{mn} h} Q_{22} - \mathrm{e}^{-\mathrm{i}\zeta^*_{mn} h} Q_{12} \right) \right\}$$

$$k_{22mn} = \frac{\mu^*(\omega_n)}{\Delta_{mn}} \left\{ \mathrm{i}\zeta^*_{mn} \left(\zeta^{*^2}_{mn} + \eta^2_m \right) \left(\eta^2_m Q_{11} Q_{22} + \xi^*_{mn} \zeta^*_{mn} Q_{12} Q_{21} \right) \right\}$$

$$k_{24mn} = \frac{\mu^*(\omega_n)}{\Delta_{mn}} \left\{ -2\mathrm{i}\zeta^*_{mn} \left(\zeta^{*^2}_{mn} + \eta^2_m \right) \left(\eta^2_m \mathrm{e}^{-\mathrm{i}\zeta^*_{mn} h} Q_{11} + \xi^*_{mn} \zeta^*_{mn} \mathrm{e}^{-\mathrm{i}\xi^*_{mn} h} Q_{21} \right) \right\}$$

Δ_{mn} is the characteristic equation of the layer element defined as

$$\Delta_{mn} = 2\eta^2_m \xi^*_{mn} \zeta^*_{mn} \left(4\mathrm{e}^{-\mathrm{i}\xi^*_{mn} h} \mathrm{e}^{-\mathrm{i}\zeta^*_{mn} h} - Q_{12} Q_{22} \right) - \left(\xi^{*^2}_{mn} \zeta^{*^2}_{mn} + \eta^4_m \right) Q_{11} Q_{21}, \text{ where}$$

$$Q_{11} = 1 - \mathrm{e}^{-2\mathrm{i}\xi^*_{mn} h}, \quad Q_{21} = 1 - \mathrm{e}^{-2\mathrm{i}\zeta^*_{mn} h}, \quad Q_{12} = 1 + \mathrm{e}^{-2\mathrm{i}\xi^*_{mn} h}, \quad Q_{22} = 1 + \mathrm{e}^{-2\mathrm{i}\zeta^*_{mn} h}$$

Stiffness matrix for an axi-symmetric half-space spectral element is:

$$\widehat{k}_{mn} = \begin{bmatrix} k_{11mn} & k_{12mn} \\ \text{sym} & k_{22mn} \end{bmatrix} \tag{A.2}$$

where

$$k_{11mn} = \frac{\mu^*(\omega_n)}{\Delta_{mn}} \mathrm{i}\xi^*_{mn} \left(\zeta^{*^2}_{mn} + \eta^2_m \right)$$

$$k_{12mn} = \frac{\mu^*(\omega_n)}{\Delta_{mn}} \eta_m \left(2\xi^*_{mn} \zeta^*_{mn} - \zeta^{*^2}_{mn} + \eta^2_m \right)$$

$$k_{22mn} = \frac{\mu^*(\omega_n)}{\Delta_{mn}} \mathrm{i}\zeta^*_{mn} \left(\zeta^{*^2}_{mn} + \eta^2_m \right)$$

in which $\Delta_{mn} = \eta^2_m + \xi^*_{mn} \zeta^*_{mn}$.

References

Achenbach, J.D., 1975. Wave Propagation in Elastic Solids. North-Holland Publishing Company, Netherlands.

Al-Khoury, R., Scarpas, A., Kasbergen, C., Blaauwendraad, J., 2001a. Spectral element technique for efficient parameter identification of layered media, Part I: Forward calculation. International Journal of Solids and Structures 38, 1605–1623.

Al-Khoury, R., Kasbergen, C., Scarpas, A., Blaauwendraad, J., 2001b. Spectral element technique for efficient parameter identification of layered media, Part II: Inverse calculation. International Journal of Solids and Structures 38, 8753–8772.

Brigham, E.O., 1998. The Fast Fourier Transform and its Applications. Prentice-Hall, Englewood Cliffs, NJ.

Doyle, J.F., 1997. Wave Propagation in Structures: Spectral Analysis using Fast Discrete Fourier Transforms. Springer-Verlag, New York.

Findley, W.N., Lai, J.S., Onaran, K., 1976. Creep and Relaxation of Nonlinear Viscoelastic Materials. North-Holland Publishing Company, Netherlands.

Hopman, P.C., 1996. The visco-elastic multilayer program VEROAD. HERON 41 (1), 71–91.

Huang, Y.H., 1993. Pavement Analysis and Design. Prentice-Hall, Englewood Cliffs, NJ.

Kolsky, H., 1963. Stress Waves in Solids. Dover Publications, New York.

Press, W.H., Flannery, B.P., Teukolsky, S.A., Vetterling, W.T., 1986. Numerical Recipes, the Art of Scientific Computing. Cambridge, Cambridge, MA.

Shames, I.H., Cozzarelli, F.A., 1992. Elastic and Inelastic Stress Analysis. Prentice-Hall, Englewood Cliffs, NJ.

van Gurp, C., 1995. Characterization of Seasonal Influences on Asphalt Pavements with the Use of Falling Weight Deflectometers. CIP, Delft.